IFUSP/P-41

High-resolution Study of the $^{118}Sn(d,p)^{119}Sn$ Reaction at 17 MeV

T.Borello-Lewin and C.Q.Orsini
and
O.Dietzsch* and E.W.Hamburger*

University of Pittsburgh, Pittsburgh Pa.,
U.S.A.

Instituto de Física
Universidade de São Paulo
BRASIL

* Permanent address: Instituto de Física, Universidade de São Paulo, C.P. 8219, S.Paulo, Brasil.

A B S T R A C T

Energy levels in ^{119}Sn up to 4.75 MeV excitation have been studied with the $^{118}Sn(d,p)\ ^{119}Sn$ reaction at an incident deuteron energy of 17 MeV. The scattered particles were analysed by a magnetic spectrograph and detected in nuclear emulsions with a resolution of ~ 9 KeV. Seventy-seven energy levels were identified. Angular distributions were compared to DWBA predictions allowing the identification of transferred angular momenta and the determination of spectroscopic factors for 49 states. The results obtained are compared with pairing theory and weak-coupling model.

1. INTRODUCTION

We have undertaken a systematic study of the odd tin isotopes, by means of (d,p) and (d,t) reactions. These nuclei have a closed proton shell, Z=50, and a large number of even stable isotopes exist and can be used as target, allowing systematic trends to be detected. Recently we published a detailed study of the ^{123}Sn, ^{113}Sn, and ^{111}Sn nuclei[1]), and a study of ^{121}Sn will be published soon[2]).

In this paper we report the results for the ^{118}Sn(d,p) ^{119}Sn reaction at 17 MeV bombarding energy. The nucleus ^{119}Sn has previously been studied by means of the same reaction by Schneid et al.[3]). The present experiment was carried out with improved energy resolution (~ 9 KeV) and more complete angular distributions, so that a number of levels previously unreported or unresolved could be observed, angular momentum and parity assignments made and spectroscopic factors determined.

2. EXPERIMENTAL PROCEDURE AND RESULTS

Targets enriched to 96.62% in ^{118}Sn were bombarded by 17 MeV deuterons from the three-stage Van de Graaff Accelerator of the University of Pittsburgh. The scattered protons were analysed in an Enge split pole magnetic spectrograph and detected in nuclear emulsions (KODAK type NTB plates, 25 μ) placed in the focal surface. Aluminium foils absorbed heavier reaction products. The emulsions were scanned at the University of São Paulo in 0.2 mm intervals along the plate. During the experiment the elastically scattered deuterons were monitored by two NaI scintillators fixed at approximately 38° relative to the incident beam.

The scattered protons were observed at 14 angles from 8^{o} to 69^{o}. Fig. 1 shows a typical spectrum. The ^{119}Sn groups are numbered and the corresponding excitations energies are given in Table 1. This table also lists, for each level, the orbital angular momenta ℓ, the tentative total spin J and parity π, the maximum experimental cross section and the spectroscopic factor determined as explained in the following section. For the $\ell=0$ transitions the experimental cross sections at the smallest angle detected are listed. For comparison, results of previous work [3,4]) are also included in table 1. The absolute cross sections are uncertain by $\pm$ 25%, while the absolute excitation energy scale is uncertain by $\pm$ 0.25%.

In the spectra, the relative distances of the peaks due to energy levels in tin isotopes, are the same (to within 0.4mm) at all angles. This fact was exploited to allow the identification of weakly excited levels. The spectra obtained at different angles were displaced until the position of the ground state peaks coincided and then summed. In the resulting "sum spectrum" peaks of tin isotopes are summed, while random background and contaminant peaks, due to light or heavy nuclei impurities in the targets,are not. From these reinforced peaks, those belonging to ^{119}Sn were identified by comparison with two spectra obtained from a "blended" target. This target contains approximately equal amounts of all even tin isotopes. However we cannot rule out entirely the presence of peaks due to contaminant nuclei of mass similar to tin.

The angular distributions obtained are shown in Figs. 2 to 8. Data for weakly excited ($\sigma_{max} \leq 0.05$mb/sr) and strongly contaminated levels were omitted.

3. DWBA ANALYSIS

Local zero-range DWBA calculations with a lower cut-off radius of 6.2fm in the radial integrals, have been performed by means of the code Julie[5]) for the analysis of the data. The optical parameters are given in Table 2 and correspond to Perey's average optical potentials for the proton[6]) and the deuteron[7]). The wave function of the captured neutrons was calculated from a potential well of Woods-Saxon shape plus a spin-orbit term.

The transferred orbital angular momentum ℓ was determined by fitting the experimental angular distributions with DWBA curves. (see Figs. 2 to 8)

The assignment of J was made from the ℓ-value, according to shell model predictions. The orbits being filled are mostly in the 50-82 neutron shell ($1g_{7/2}$,$2d_{5/2}$,$2d_{3/2}$,$3s_{1/2}$,$1h_{11/2}$). For ℓ=2 there is an ambiguity and assignments were made by comparing ratios of cross sections for (p,d)[4]) and (d,p) reactions[3]). For the levels having ℓ=1 and ℓ=3 the assignments J=3/2 and J=7/2 were made tentatively.

The spectroscopic factors S_{dp} were obtained in the usual fashion by comparing experimental and calculated differential cross sections, near the first maximum in the angular distributions.

4. COMMENTS ON THE OBSERVED LEVELS

Shown in table 1 are many weak levels which have not been observed in previous work. The detection and identification of states with very small cross-sections have been made

possible mainly because of the technique employed of summing spectra at different angles and comparing the yield obtained with the enriched target to the yield produced by the "blended" target. This latter method is very powerful in discriminating levels which belong to other tin isotopes. In a few instances however the yield of a given level is not in complete agreement with the expected contaminant group as observed in spectra taken with the blended target. In such cases when an unambiguous discrimination could not be made the states were included in the table on a tentative basis and the level numbers are written in a parenthesis (see also footnote a in table 1). Levels which are suspect of consisting of unresolved doublets are also indicated.

Orbital angular momentum assignments which are tentative are also indicated in parenthesis in table 1. In cases where the angular distributions can be equally fitted with more than one ℓ-value (e.g., level no. 42 at E_x=3.595 MeV) both curves are displayed in the corresponding figures. For the levels at 3.891 and 3.955 MeV, ℓ=1 assignments were made on a very tentative basis on the grounds that slightly better fits are obtained to the data with ℓ=1 than with ℓ=3 curves.

We detected in the present work all the states seen by Schneid et al.[3]) in the reactions ^{118}Sn(d,p) and ^{120}Sn(d,t) with 15 MeV deuterons and ~ 40 keV resolution. The only exception is their level at 3.23 MeV. In our spectra a peak appears at the expected position but corresponds to a state that belongs to ^{121}Sn. There is however a systematic discrepancy of ~ 40 keV between our excitation energies and the energies quoted by Schneid et al.[3]). Four levels (at 2.21,2.40,

2.47 and 3.01 MeV) reported by Cavanagh et al.[4]) in their study of the ^{120}Sn(d,p) reaction at $E_p \simeq 30$ MeV were not observed in the present work.

While most of the ℓ-values extracted in the present work agree with those reported in these two earlier studies[3,4])there are serious discrepancies for a few strong states. Thus, the three ℓ=1 states reported by Schneid et al.[3]) at 1.95, 2.92 and 3.13 MeV, show up in our data as states with ℓ=2, 2 and 3, respectively. On the other hand our results clearly indicate that the p strength is concentrated between ~ 3.5 and ~ 4.5 MeV, a region of excitation energies which was not examined in previous studies.

The level at 2.636 has been assigned ℓ=2 by Cavanagh et al.[4]). Our angular distribution could be fitted either with ℓ=2 or ℓ=3 curves. The assignment ℓ=3 was made because from a comparison of the (d,p) cross section with the (p,d) cross section of ref. 4 a ratio resulted that is one order of magnitude higher than a typical ratio for a $\frac{5+}{2}$ or a $\frac{3+}{2}$ state.

The level that we observe at 922 keV is known from the Coulomb excitation study of Stelson et al.[8]) and from the decay of ^{119}Sn investigated by Raman et al.[9]) and Jacobs et al.[10]) to be a close doublet at 920.5 and 921.4 keV with spins $\frac{3+}{2}$ and $\frac{5+}{2}$, respectively. With the exception of this unresolved doublet and the level at 1.3044 MeV reported by Raman et al.[9]), which we do not observe, there is good agreement between our results and the results of these high resolution gamma-ray investigations[9,10]).

On the other hand, we did not observe a few levels that were identified in the ^{118}Sn(n,γ) reaction. They are the states

at 1.773, 2.292 and 2.397 MeV reported by Samour et al.[11]) and the level at 1.778 MeV seen by Bhat et al.[12]).

Quite large discrepancies exist between the spectroscopic factors extracted in the present work and those quoted in the work of Schneid et al.[3]) even for the strong states. A striking example is the ℓ=0 transition to the ground state for which our spectroscopic factor is half the value found by Schneid et al.[3]). For the weak states the discrepancies can be as large as a factor of 3. The origins of such differences are difficult to ascertain.

5. COMPARISON OF RESULTS WITH THEORETICAL PREDICTIONS

5.1 - Pairing Theory

The low lying states of the odd tin nuclei have a significant one quasiparticle (1QP) component. The 1QP energy $E_{\ell j}$ relative to the ground state can be defined as the "excitation energy center of gravity", with each state weighted by its probability of including the corresponding single particle level, be it as a particle or as a hole[13]).

In this work, the 1QP energies were estimated considering only the contributions of states detected in the (d,p) reaction and were calculated from the experimental excitation energies $E_i(\ell,j)$ and corresponding spectroscopic factors, according to the relation:

$$E_{\ell j} = \frac{\Sigma_i S_{i,dp}(\ell,j) E_i(\ell,j)}{\Sigma_i S_{i,dp}(\ell,j)}$$

were the summation includes all the identified (ℓ,j) states and

the denominator represents the experimental non-occupation probability (U_j^2) of each nℓj single particle level of the target nucleus.

The obtained 1QP energies $E_{\ell j}$, non-occupation probabilities U_j^2 and the number of neutron holes $(2j+1)U_j^2$ for ^{118}Sn are given in table 3. The total number of neutron holes in the N=50-82 shell should be 14 under the assumption that the next shell is empty and the lower one completely full. Experimentally we found 13.9.

Fig. 9 shows the spectroscopic strengths as a function of excitation energy obtained for each ℓj and the respective center of gravity. The heights of the lines are proportional to the spectroscopic factor. For the center of gravity this height is proportional to the sum of all spectroscopic factors, It can be seen that the low lying single-particle levels show a very little fractioning. The same certainly is not true for the high lying $p_{3/2}$ and $f_{7/2}$ states. The spreading of the strength for these states is in reasonable agreement with the widths expected from the prescription by Cohen et al.[14]) that the half width of the distribution should be approximately $\frac{1}{3}$ E*, where E* is taken to be the single-particle energy.

According to pairing theory[15]), the quasiparticle energies are given by

$$E_{\ell j} - E_{\ell o j o} = \{(e_{\ell j} - \lambda)^2 + \Delta^2\}^{1/2} - \{(e_{\ell_o j_o} - \lambda)^2 + \Delta^2\}^{1/2} \quad (1)$$

and

$$\Sigma_i S_{i,dp}(\ell,j) = \frac{1}{2}\left\{1 + \frac{e_{\ell j} - \lambda}{\left[(e_{\ell j} - \lambda)^2 + \Delta^2\right]^{1/2}}\right\} \quad (2)$$

where: $(e_{\ell j} - \lambda)$ and $(e_{\ell_o j_o} - \lambda)$ are the energies of the single particle levels nℓj and $n_o \ell_o j_o$, measured relative to the Fermi

surface; Δ is the energy gap and in practice is given by the the odd-even mass difference (Δ = 1.31 MeV[16]).

A comparison of theory and experiment is shown in fig.10. The full curve was obtained from eq. 2 treating $(e_{\ell j} - \lambda)$ and $\Sigma S_{i,dp}$ as continuous variables. The horizontal bars, on the other hand, show the experimental value of $\Sigma S_{i,dp}$ and the position of each single particle level. This position was calculated from eq. 1 using the value of $(e_{\ell_o j_o} - \lambda)$ corresponding to the lowest center of gravity, predicted by eq. 2 with the experimental value of $\Sigma\ S_{i,dp}(\ell_o, j_o)$.

The $11/2^-$ and $3/2^+$ levels are above the fermi surface (FS). The closing of the 50-82 shell is responsible for the large gap between the $3/2^+$ level and the next one. The $7/2^-$ and $3/2^-$ levels are quite far from the fermi surface. Only lower limits of $\Sigma S_{i,dp}$ were obtained in these cases, since some of the strength is probably located at excitation energies above ~ 4,8 MeV and was not detected in this experiment.

5.2 - Weak -coupling model

According to the weak-coupling model[17]) the interaction of low-lying 1QP - states(such as $s_{1/2}$, $d_{3/2}$ and $h_{11/2}$ in our case) with the 2^+ phonon should produce multiplets of states with energies above the 1QP level that are equal, to first approximation, to the phonon excitation energy. We should therefore expect to observe states in ^{119}Sn at excitation energies around 1.1 MeV which should show "collective" properties. In fact the doublet of states at 920 keV which is strongly populated in Coulomb excitation[8]) has been interpreted as resulting from the coupling of a $s_{1/2}$ neutron

to the one phonon 2^+ excitation of the core. If these states contain significant single particle amplitudes in the wave functions they should be detectable in a (d,p) reaction.

We have identified a negative parity state which can be attributed to the coupling of a $h_{11/2}$ quasiparticle to the 2^+ phonon state, namely the 1.062 MeV ℓ=3 level in ^{119}Sn. Similar states are also observed in the nuclei ^{117}Sn, ^{121}Sn, ^{123}Sn and ^{125}Sn (references 18, 1, 2, 19) and have been the subject of weak-coupling calculations[20,21]). There is appreciable mixing with the $1f_{7/2}$ single particle state and it is this single particle component which is seen in the (d,p) reaction. The calculations[20,21]) bear out this interpretation. The theoretical results reported in ref. 21, moreover, point outo to the importance of taking into account ground state correlations.

6. CONCLUSIONS

A total of 77 states in ^{119}Sn were identified in the present work up to an excitation energy of 4.758 MeV. The fact that about two thirds of them were not reported before is due to the poorer energy resolution employed in previous studies[3,4]) and smaller ranges of excitation energies investigated by those authors. From a comparison of the angular distributions taken over a wide interval of angles to the predictions of the DWBA calculations, we were able to assign orbital angular momentum and extract spectroscopic factors for 49 of the detected states.

The sum of spectroscopic factors and the centers of gravity for the levels with same spin and parity are in good agreement with the values predicted by the pairing theory for

the levels in the neutron shell between N=50 and N=82. Some of the strength in the $f_{7/2}$ and $p_{3/2}$ levels of the next major shell was also located.

The high resolution employed in the present study and the careful search for weakly excited states leads to the belief that the distribution of 1QP strengths among levels in ^{119}Sn up to 4.5 MeV in excitation is now quite well established. From the presence of a low lying 2^+ state in the neighbouring even isotopes, however, one can expect three quasiparticle (3QP) states starting at about 1 MeV. It would therefore be highly desirable to compare the level spectrum as determined in the present one-nucleon transfer experiment with what would be obtained in a high resolution (t,p) experiment to locate the three quasiparticle component admixtures.

We gratefully acknowledge the support of Prof.B.L. Cohen at the University of Pittsburgh. We would also like to thank the microscopists who read the plates. Financial support from Fundação de Amparo à Pesquisa do Estado de São Paulo, Banco Nacional do Desenvolvimento Econômico and Conselho Nacional de Pesquisas is also acknowledged.

FIGURE CAPTIONS

Fig. 1 - Proton spectrum from the $^{118}Sn(d,p)$ ^{119}Sn reaction. The ^{119}Sn groups are numbered. The two strong and broad peaks are due to light mass impurities in the target.

Fig. 2 - Angular distributions of proton groups from the ^{118}Sn (d,p) ^{119}Sn reaction. Transferred angular momentum ℓ, excitation energy E_x (in MeV) and DWBA predicted curves are indicated.

Fig. 3-4-5-6-7-8 - See caption for Fig. 2

Fig. 9 - Fragmentation of single-particle strengths among levels belonging to the same shell-model state in ^{119}Sn. The height of each line is proportional to the spectroscopic factor for each level.

Fig. 10- Comparison of the summed spectroscopic factors (heavy horizontal lines) with the prediction from pairing theory (full curve) given by Eq.(2).

REFERENCES

1. T.Borello, E.Frota Pessoal, C.Q.Orsini, O.Dietzsch and E.W.Hamburger, Rev. Bras. Fis. 2 (1972) 157.
2. M.J.Bechara, Master Thesis, Instituto de Física, Univ. São Paulo,1973, M.J.Bechara and O. Dietzsch to be published.
3. E.J.Schneid, A.Prakash and B.L.Cohen, Phys.Rev. 156 (1967) 1316.
4. P.E.Cavanagh, C.F.Coleman, A.G.Hardacre, G.A.Gard and J.F. Turner, Nucl.Phys. A141 (1970)97.
5. R.H. Bassel, R.M.Drisko and G.R.Satchler, ORNL Report(1966) nº 3240.
6. F.G.Perey, Phys. Rev. 131 (1963) 745.
7. C.M.Perey and F.G.Perey, Phys.Rev. 132 (1963) 755.
8. P.H.Stelson, W.T.Milner, F.K.Mcgowan, R.L.Robinson and S.Raman, Nucl.Phys. A190 (1972)197.
9. S.Raman, P.H.Stelson, G.G.Slaughter, J.A.Harvey,T.A.Walkiewicz, G.J.Lutz, L.G.Multhauf and K.G.Tirsell, Nucl.Phys. A206 (1973)343.
10. E.Jacobs and D. De Frenne, Z. Physik 257 (1972) 402.
11. C. Samour, J.Julien, J.M. Kuchly, R.N.Alves and J. Morgenstern, Nucl.Phys., A122 (1968) 512.
12. M.R.Bhat, R.E.Chrien, O.A.Wasson, M.Beer and M.A.Lone, Phys. Rev. 166 (1968) 1111.
13. M. Baranger, Nucl.Phys. A149 (1970)225.
14. B.L.Cohen, R.H.Fulmer and A.L.McCarthy, Phys.Rev.126 (1962) 698.
15. M. Baranger, Phys.Rev. 120 (1960)957.
16. N.B.Gove and A.H.Wapstra - Nucl.Data Tables 11A (1972) 127.
17. A. de Shalit, Phys.Rev. 122 (1961) 1530.
18. L. Goldman and B.L.Cohen, private communication.
19. C.R.Bingham and D.L.Hillis, Phys.Rev. 8C(1973) 729.
20. M.J.Bechara, T.Borello Lewin, O.Dietzsch, E.W.Hamburger, H.Miyake and A.F.R.T.Piza, Proceedings of the International Conference on Nuclear Physics, Munchen 1973, Vol. 1, p.224 (North-Holland Publ. Co. 1973).
21. S. de Barros, M.J.Bechara, T.Borello-Lewin and V.Paar, Phys. Lett. 49B (1974) 113.

T A B L E 1

LEVEL NUMBER	RESULTS OF THE PRESENT EXPERIMENT E_d = 17 MeV					SCHNEID Et Al[3] E_d = 15 MeV (d,p)				(d,t)	CAVANAGH Et Al[4] E_p = 30MeV (p,d)		
	Ex (MeV)	ℓ	J^π	$(\frac{d\sigma}{d\Omega})_{max}$ (mb/sr)	S_{dp}	Ex (MeV)	ℓ	J^π	S_{dp}	Ex (MeV)	Ex (MeV)	ℓ	J^π
0	0	0	$1/2^+$	3.4[c]	0.29	0	0	$1/2^+$	0.59	0	0	0	$1/2^+$
1	0.024	2	$3/2^+$	4.6	0.52	0.024	2	$3/2^+$	0.52	0.030	0.021	2	$3/2^+$
2	0.089	5	$11/2^-$	1.5	0.69	0.08	5	$11/2^-$	0.56	0.08	0.088	5	$11/2^-$
3	0.788	4	$7/2^+$	0.16	0.059	0.79	4	$7/2^+$	0.14	0.78	0.790	4	$7/2^+$
4	0.922	2	$5/2^+$	0.15	0.009	0.93	2	$5/2^+$	0.006	0.92	0.922	2	$5/2^+$
5	1.062	3	$(7/2^-)$	0.39	0.034								
6	1.088	2	$5/2^+$	2.3	0.14	1.10	2	$5/2^+$	0.084	1.08	1.096	2	$5/2^+$
7	1.186	2	$3/2^+$	0.25	0.021	1.22	2	$5/2^+$	0.008	1.24			
8	1.248	0	$1/2^+$	0.15[c]	0.011						1.25		
9	1.309	(2)	$(5/2^+)$	0.05	0.003								
10	1.354	2	$5/2^+$	0.35	0.021	1.37	2	$5/2^+$	0.014		1.368	2	$5/2^+$
11	1.553	2	$3/2^+$	0.20	0.017	1.59	2	$5/2^+$	0.007	1.56	1.57	2	$3/2^+$
12	1.631	2	$5/2^+$	0.05	0.003					1.64	1.64	2	$3/2^+,5/2^+$
13	1.715	2	$(5/2^+)$	0.14	0.007	1.74	2	$5/2^+$	0.011	1.73	1.74	2	$3/2^+$
14	1.905	2	$(5/2^+)$	0.19	0.008	1.95	(1)	$(3/2^-)$	0.011		1.95		
15	2.120	0	$1/2^+$	0.20[c]	0.011						2.137		$1/2^+$
											2.21	2	$3/2^+,5/2^+$
16	2.258	2	$(5/2^+)$	0.06	0.003								
17	2.322	2	$3/2^+$	0.08	0.006						2.32		
18	2.367	2	$(5/2^+)$	0.20	0.011						2.40	5	$11/2^-$
											2.47		
19	2.549	3	$(7/2^-)$	0.81	0.047	2.58	(1,2)	$(3/2^-,5/2^+)$	0.014,0.025		2.54		
20	2.636	(3)	$(7/2^-)$	1.5	0.090	2.68	(3)	$(7/2^-)$	0.12		2.64	(2)	$(3/2^+)$
21	2.723[b]			0.07							2.71	1	
(22)[a]	2.771[b]			0.06									
(23)[a]	2.813			0.04									
24	2.823		$(3/2^+)$	≥0.05									
25	2.846	2	$(5/2^+)$	0.49	0.032						2.84	1	
26	2.874	2	$(3/2^+)$	0.75	0.034								
27	2.900	2	$(5/2^+)$	0.51	0.034	2.92	(1)	$(3/2^-)$	0.057		2.89	(2)	$(3/2^+)$
28	2.939	2		0.46	0.021								
29	2.965[b]			0.25									
											3.01	2	$3/2^+$
30	3.071	2	$(5/2^+)$	0.84	0.035								
31	3.093	3	$(7/2^-)$	0.48	0.025	3.13	(1)	$(3/2^-)$	0.046				
32	3.158	3	$(7/2^-)$	0.86	0.045								
33	3.191			≥0.15									
						3.23	(3)	$(7/2^-)$	0.089				
34	3.279	2	$(5/2^+)$	0.76	0.032	3.33	(3)	$(7/2^-)$	0.037				
35	3.366			≥0.15									
36	3.375	(2,3)	$(5/2^+,7/2^-)$	0.53	0.025,0.027								
37	3.389			≥0.13									
38	3.442	1	$(3/2^-)$	0.44	0.013								
39	3.481	1	$(3/2^-)$	0.70	0.028	3.54	(3)	$(7/2^-)$	0.086				
40	3.527	1	$(3/2^-)$	0.50	0.019								
41	3.566	1	$(3/2^-)$	0.35	0.013								
42	3.595	(1,3)	$(3/2^-,7/2^-)$	0.28	0.015,0.014								
43	3.618	1	$(3/2^-)$	0.77	0.026	3.67	(3)	$(7/2^-)$	0.118				
44	3.656	1	$(3/2^-)$	0.52	0.019								
(45)[a]	3.675			≥0.10									
(46)[a]	3.690			≥0.05									
47	3.730			0.13									
48[a]	3.770			0.77									
49	3.807	1	$(3/2^-)$	1.7	0.075	3.87	(3)	$(7/2^-)$	0.146				
50	3.843	1	$(3/2^-)$	0.55	0.026								
(51)[a]	3.880			0.11									
(52)[a]	3.891	(1)	$(3/2^-)$	0.13	0.005								
(53)[a]	3.905			≥0.05									
54	3.921	3	$(7/2^-)$	0.20	0.008								
55	3.955	(1)	$(3/2^-)$	0.66	0.034								
56	3.987			≥0.50									
57	4.031			≥0.15									
58	4.062	1	$(3/2^-)$	0.49	0.019								
59	4.115			≥0.10									
60	4.138			0.23									
61	4.191			≥0.10									
62	4.210			≥0.10									
63	4.235	3	$(7/2^-)$	0.17	0.006								
64	4.261	3	$(7/2^-)$	0.24	0.009								
65	4.301	(1)	$(3/2^-)$	0.38	0.014								
66	4.350			≥0.30									
67	4.380	1	$(3/2^-)$	0.82	0.037								
68	4.418			≥0.15									
69	4.435			≥0.10									
70	4.451			≥0.15									
71	4.521			≥0.10									
72	4.552	(3)	$(7/2^-)$	0.58	0.019								
73	4.610	(1)	$(3/2^-)$	0.20	0.007								
74	4.663			≥0.05									
75	4.688			≥0.15									
76	4.758			≥0.15									

a) This level may arise from the presence of other tin isotopes in the target. Its yield, however, is not in complete agreement with the expected contaminant group as observed in spectra taken with the bleached target (see text). Since an unambiguous discrimination could not be made, the state was included in the table on a tentative basis.

b) The experimental evidence suggests that this level may be an unresolved doublet.

c) For a ℓ =0 transition, the cross section at $\theta=8^\circ$ is listed.

Table 2 - Optical model parameters used in DWBA calculations

	Deuteron	Bound Neutron	Proton
r_c(fm)	1.15		1.25
V(MeV)	97.4	a)	53.0
r_o(fm)	1.15	1.25	1.25
a(fm)	0.81	0.65	0.65
W(MeV)	0		0
W'(MeV)	18.5		13.5
r_o'(fm)	1.34		1.25
a'(fm)	0.68		0.47
V_{so}(MeV)	0	λ_{so}=25	7.5

a) Adjusted to reproduce the neutron binding energy.

Table 3 - 1QP energies $E_{\ell j}$, non-occupation probabilities U_j^2 and number of neutron holes $(2j+1)U_j^2$ for ^{118}Sn

J^π	$E_{\ell j}$ (MeV)	U_j^2	$(2j+1)U_j^2$
$5/2^+$	1.921	0.33	1.98
$7/2^+$	0.788	0.06	0.48
$1/2^+$	0.124	0.31	0.62
$3/2^+$	0.428	0.63	2.52
$11/2^-$	0.094	0.69	8.28
$7/2^-$	>2.856	0.31	-
$3/2^-$	>3.840	0.35	-

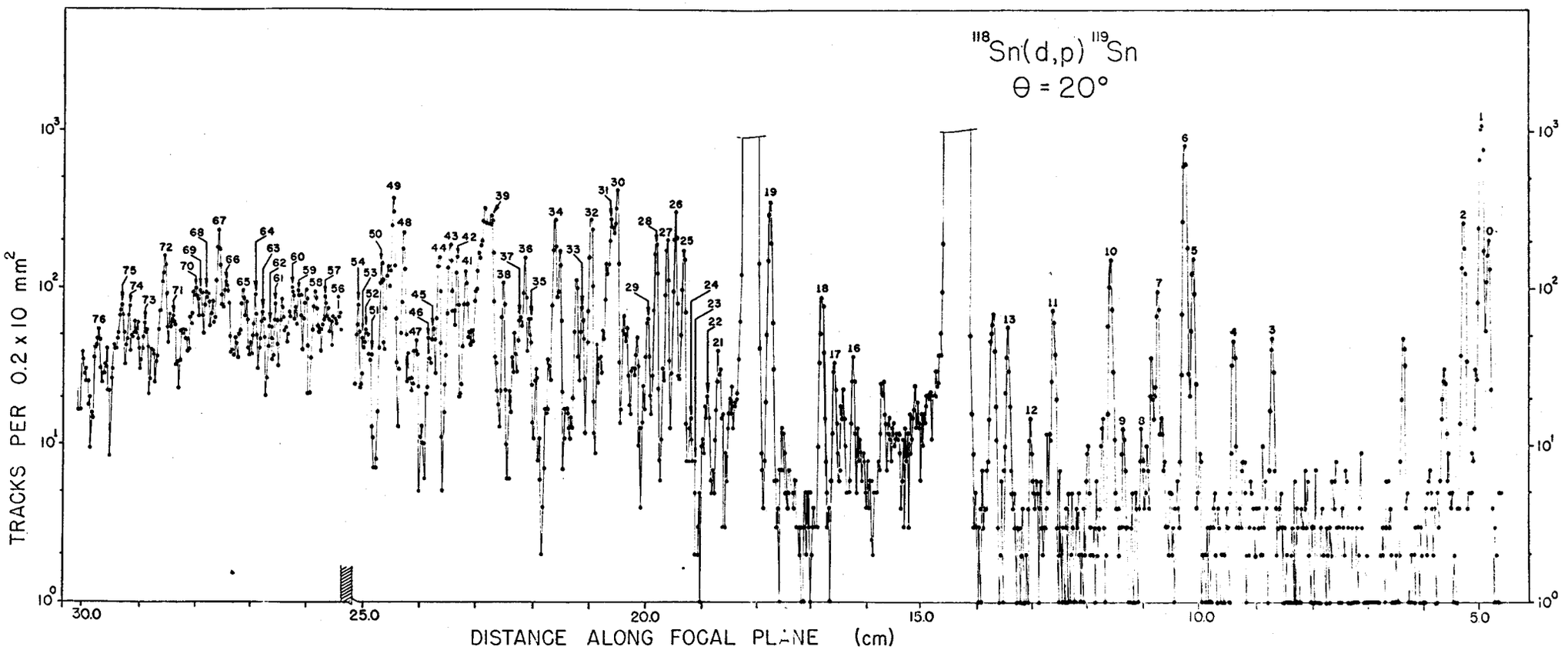
$^{118}Sn(d,p)^{119}Sn$
$\theta = 20°$
TRACKS PER 0.2 x 10 mm^2
DISTANCE ALONG FOCAL PLANE (cm)
30.0
25.0
20.0
15.0
10.0
5.0
10^0
10^1
10^2
10^3

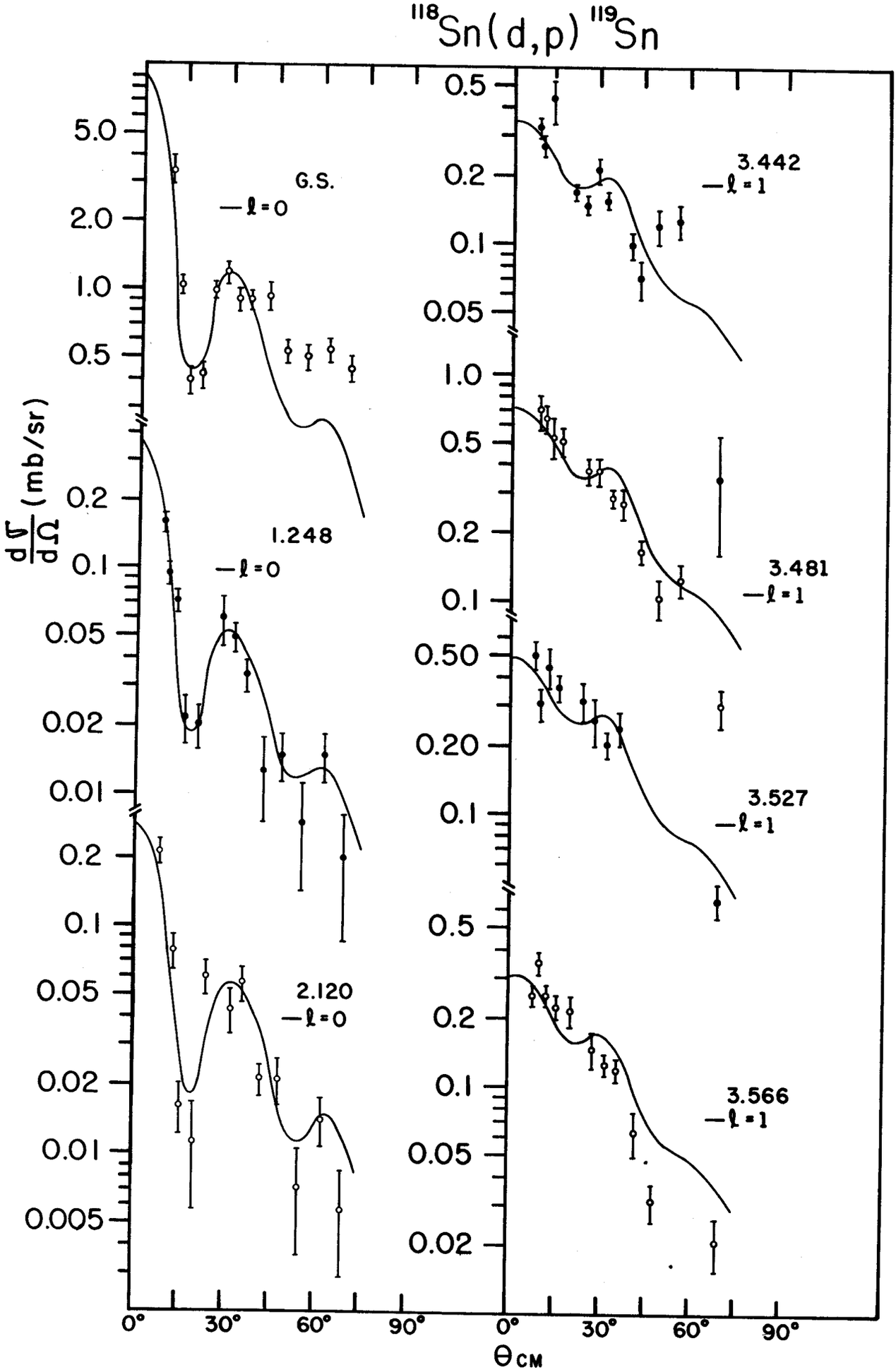
$^{118}Sn(d,p)^{119}Sn$
G.S.
—ℓ=0
1.248
—ℓ=0
2.120
—ℓ=0
3.442
—ℓ=1
3.481
—ℓ=1
3.527
—ℓ=1
3.566
—ℓ=1
$\frac{d\sigma}{d\Omega}$ (mb/sr)
θ_{CM}
0°
30°
60°
90°

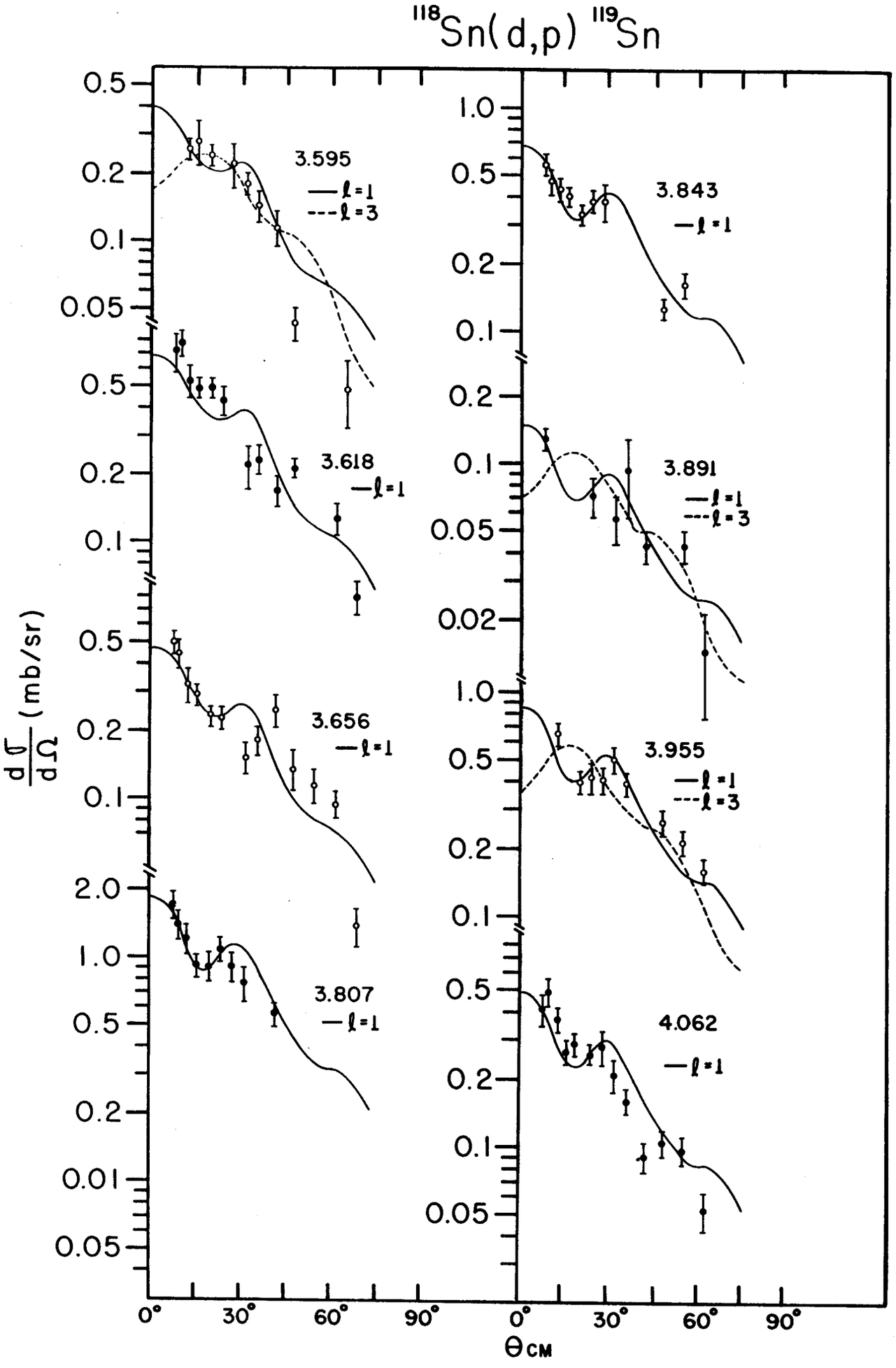
^{118}Sn(d,p) ^{119}Sn
3.595
ℓ=1
ℓ=3
3.618
ℓ=1
3.656
ℓ=1
3.807
ℓ=1
3.843
ℓ=1
3.891
ℓ=1
ℓ=3
3.955
ℓ=1
ℓ=3
4.062
ℓ=1
dσ/dΩ (mb/sr)
θcm
0°
30°
60°
90°

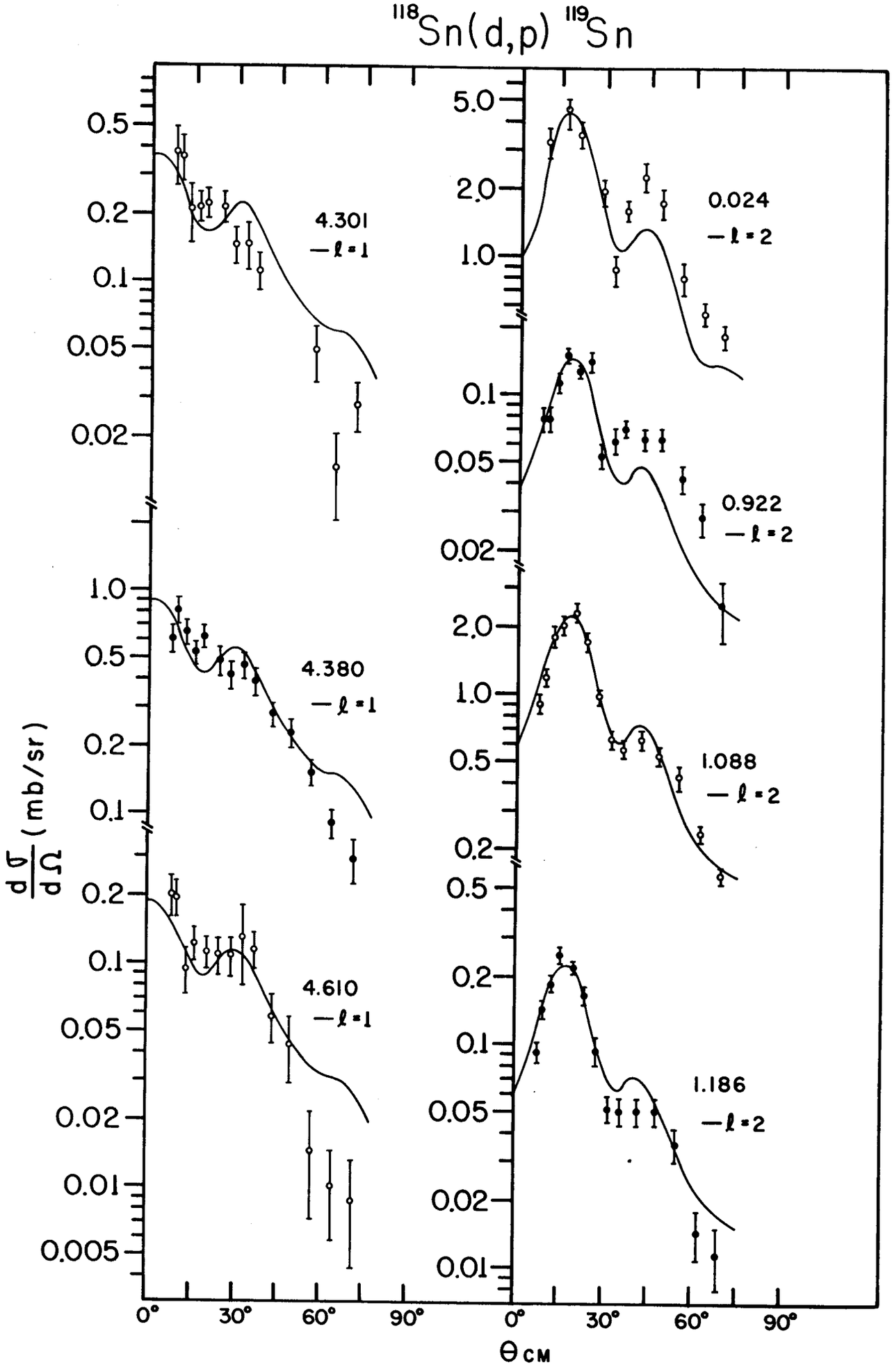
$^{118}Sn(d,p)\ ^{119}Sn$
4.301
$-\ell=1$
4.380
$-\ell=1$
4.610
$-\ell=1$
0.024
$-\ell=2$
0.922
$-\ell=2$
1.088
$-\ell=2$
1.186
$-\ell=2$
$\frac{d\sigma}{d\Omega}$ (mb/sr)
θ_{CM}
0°
30°
60°
90°

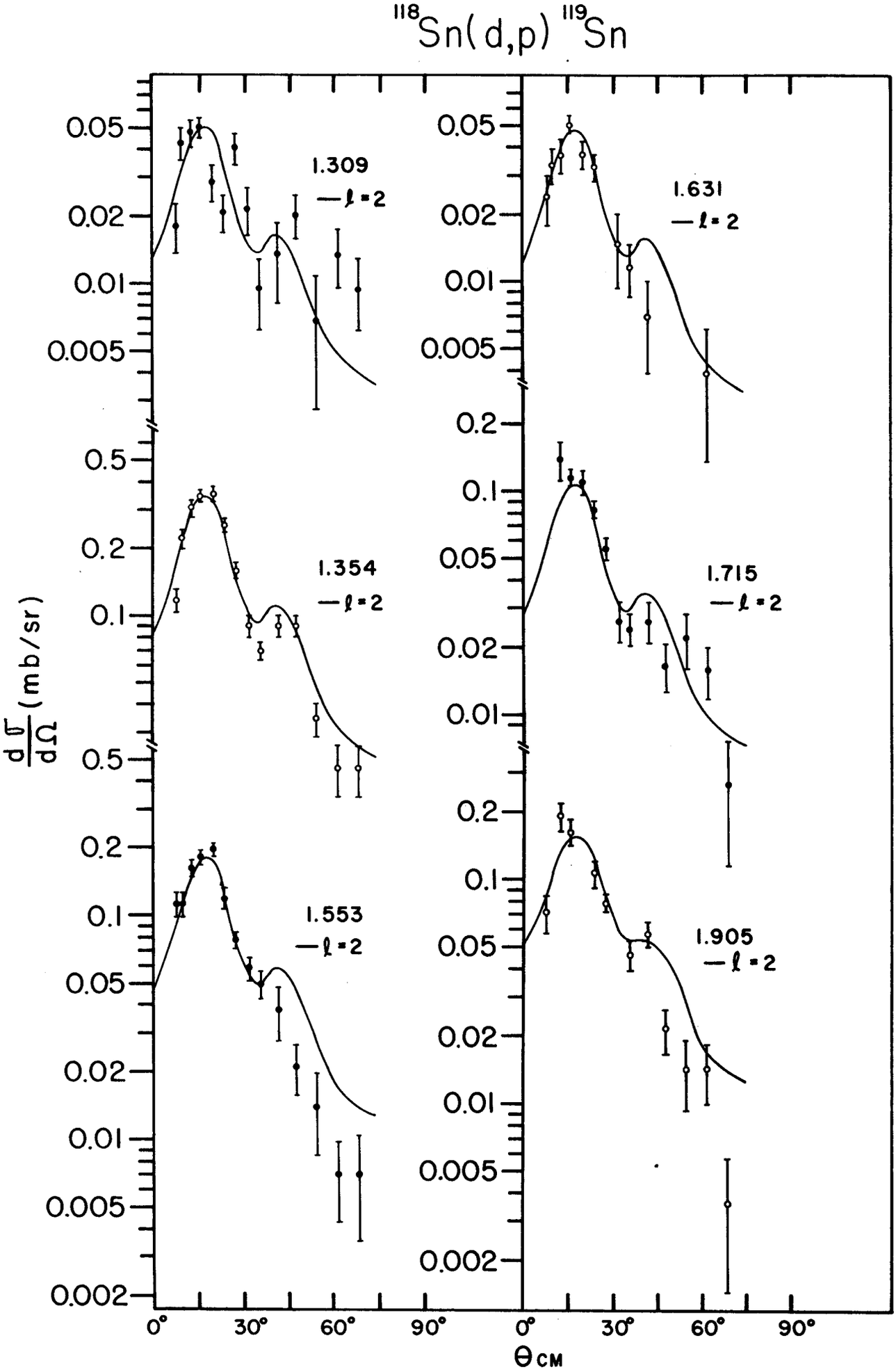
118Sn(d,p) 119Sn
1.309
—ℓ=2
1.631
—ℓ=2
1.354
—ℓ=2
1.715
—ℓ=2
1.553
—ℓ=2
1.905
—ℓ=2
dσ/dΩ (mb/sr)
0.05
0.02
0.01
0.005
0.5
0.2
0.1
0.05
0.02
0.01
0.2
0.1
0.05
0.02
0.01
0.005
0.002
0.2
0.1
0.05
0.02
0.01
0.005
0.002
0°
30°
60°
90°
0°
30°
60°
90°
θ CM

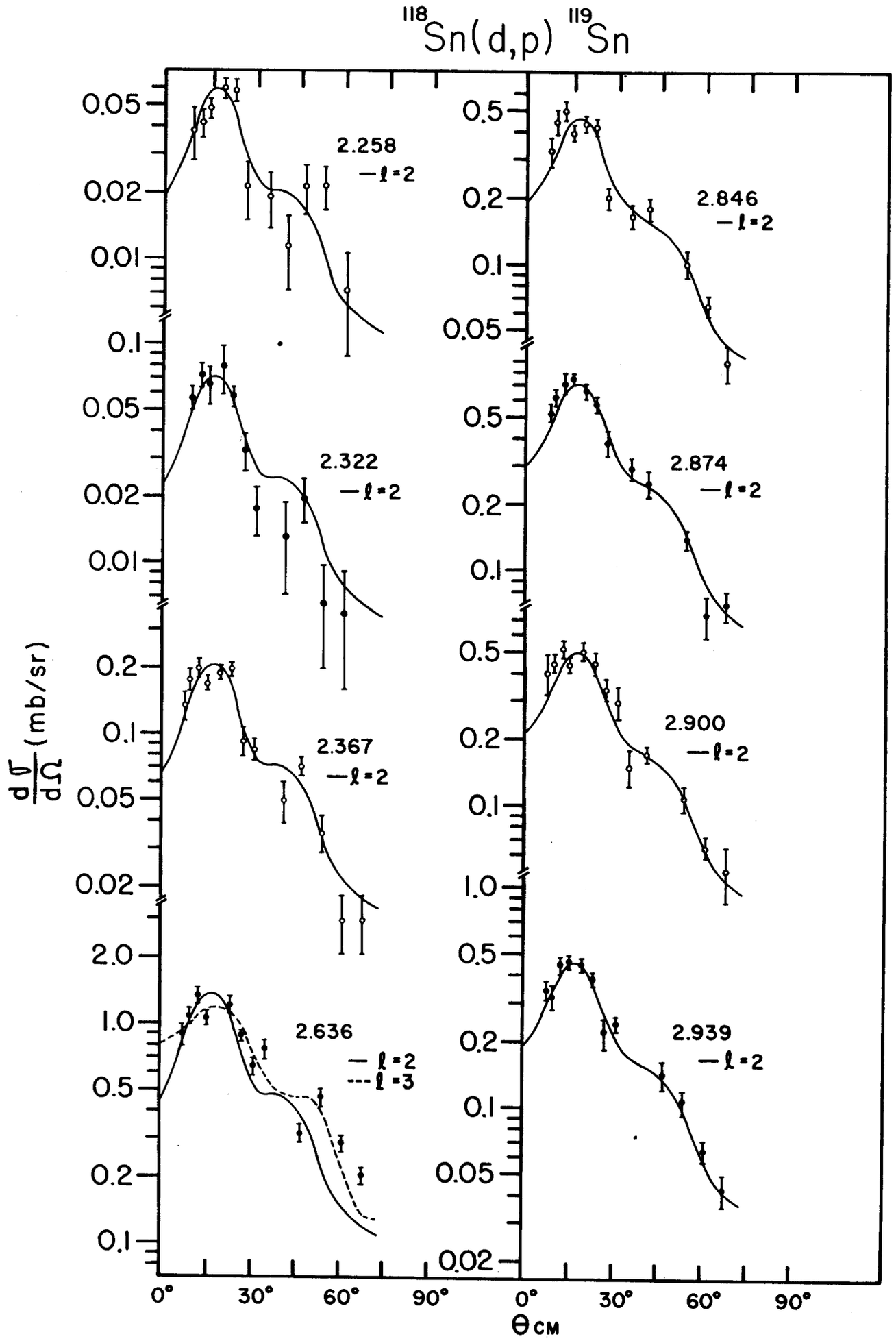
118Sn(d,p) 119Sn
2.258
—l=2
2.322
—l=2
2.367
—l=2
2.636
— l=2
--- l=3
2.846
—l=2
2.874
—l=2
2.900
—l=2
2.939
—l=2
dσ/dΩ (mb/sr)
θ CM
0°
30°
60°
90°

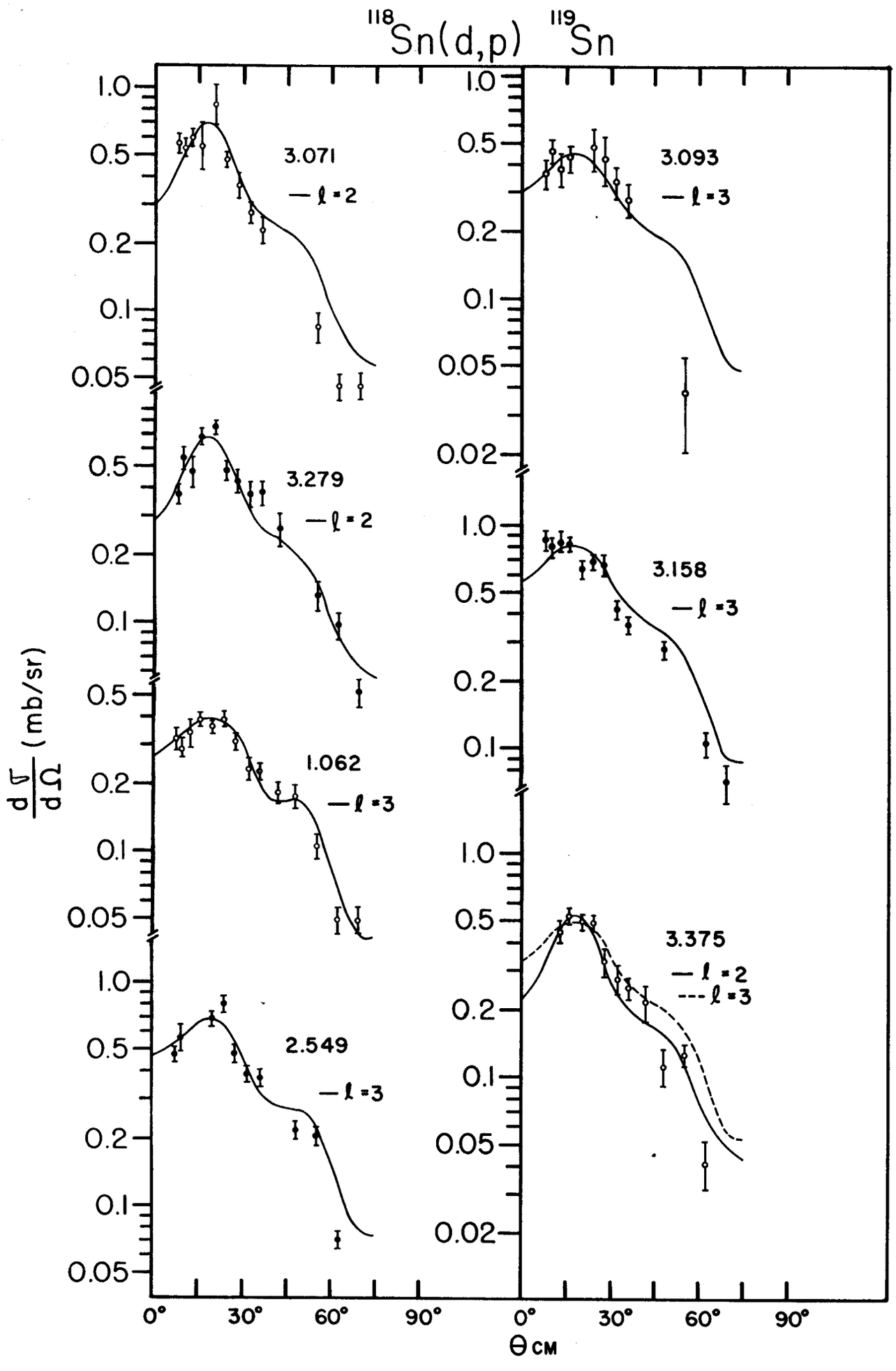
^{118}Sn(d,p) ^{119}Sn
3.071
— ℓ = 2
3.093
— ℓ = 3
3.279
— ℓ = 2
3.158
— ℓ = 3
1.062
— ℓ = 3
3.375
— ℓ = 2
--- ℓ = 3
2.549
— ℓ = 3
dσ/dΩ (mb/sr)
θ CM
0°
30°
60°
90°

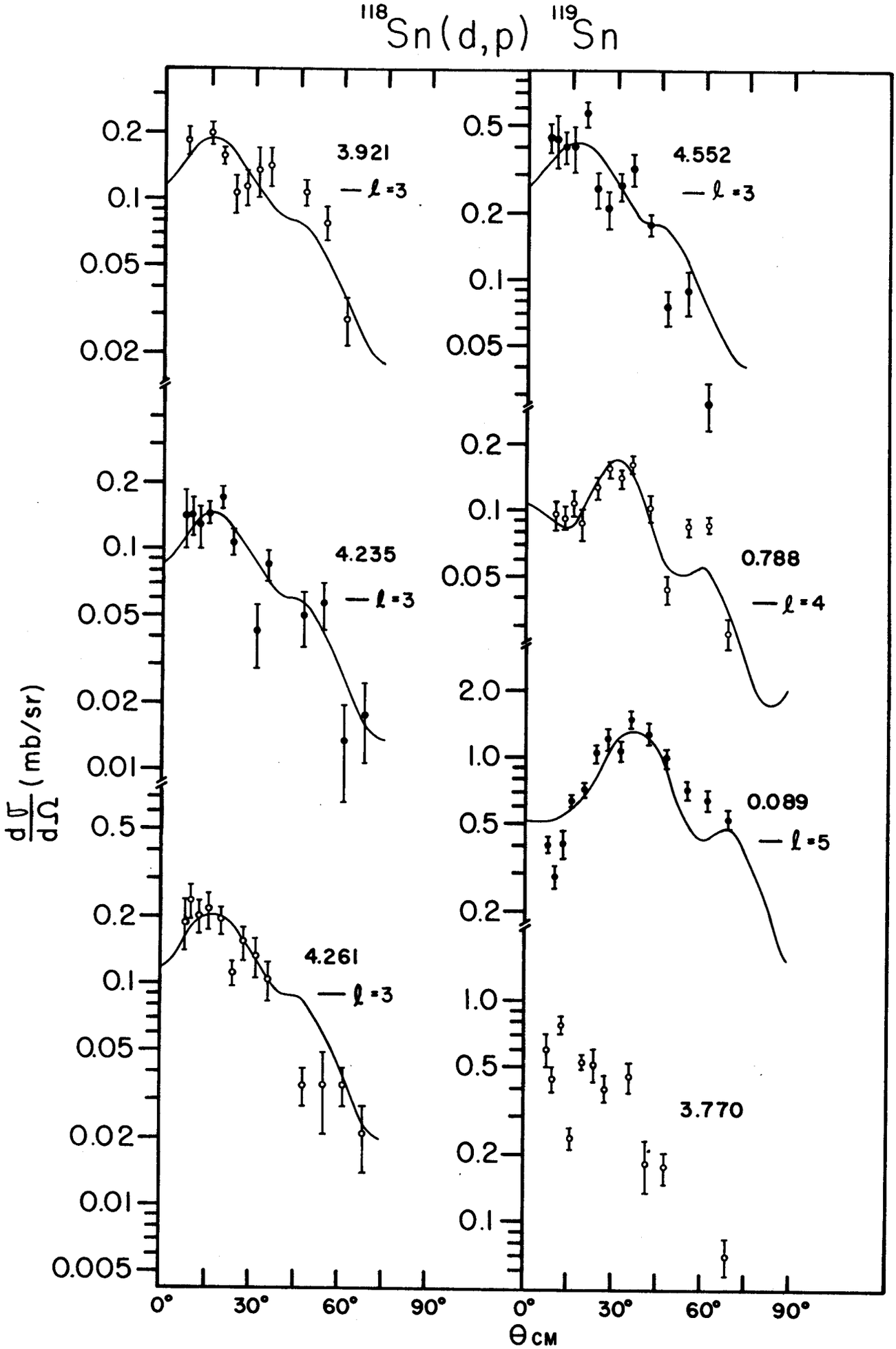
^{118}Sn(d,p) ^{119}Sn
3.921
— ℓ=3
4.552
— ℓ=3
4.235
— ℓ=3
0.788
— ℓ=4
4.261
— ℓ=3
0.089
— ℓ=5
3.770
dσ/dΩ (mb/sr)
θ CM
0°
30°
60°
90°

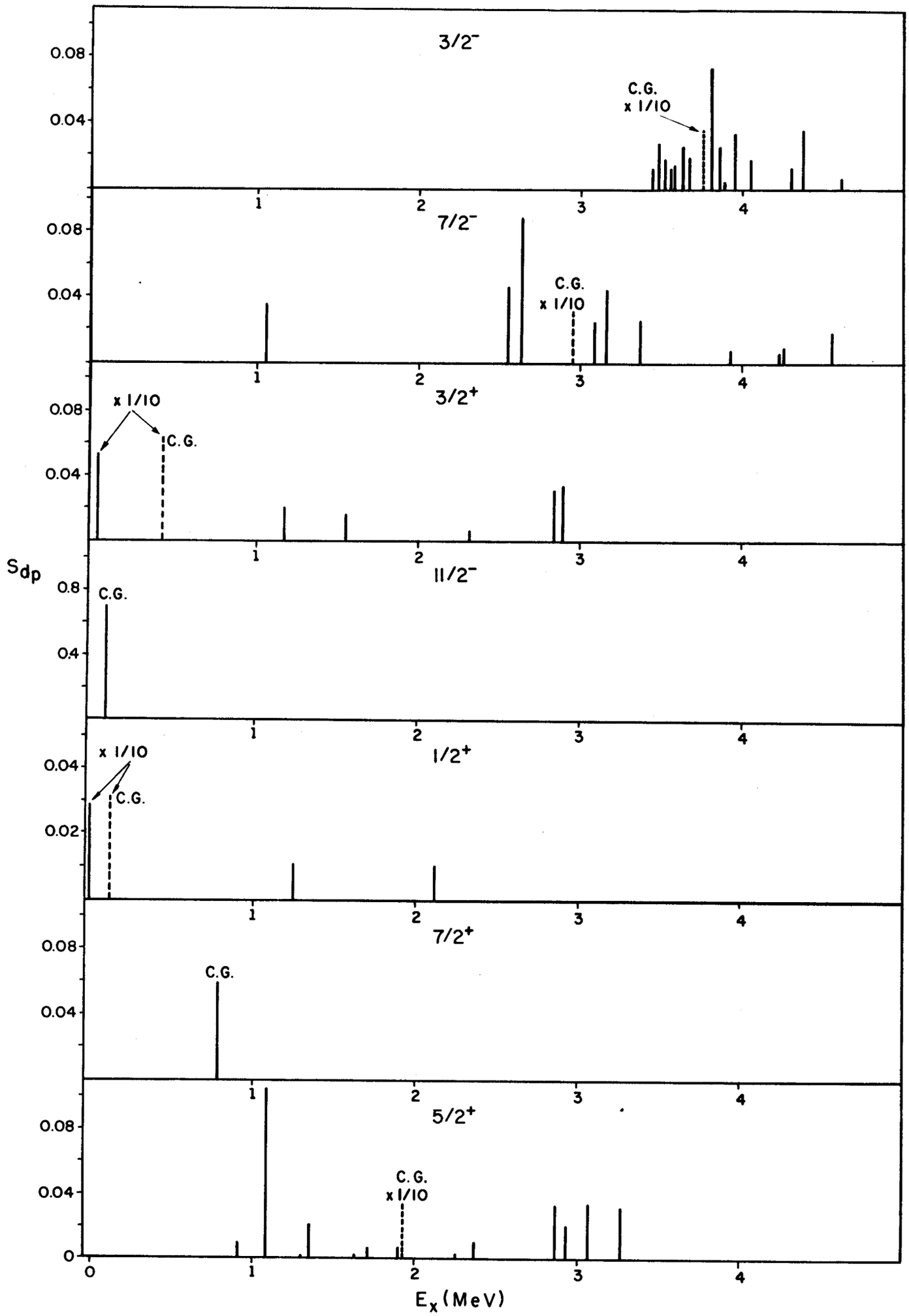
3/2⁻
C.G.
x 1/10
7/2⁻
C.G.
x 1/10
3/2⁺
x 1/10
C.G.
11/2⁻
C.G.
1/2⁺
x 1/10
C.G.
7/2⁺
C.G.
5/2⁺
C.G.
x 1/10
Sdp
Ex (MeV)

^{118}Sn

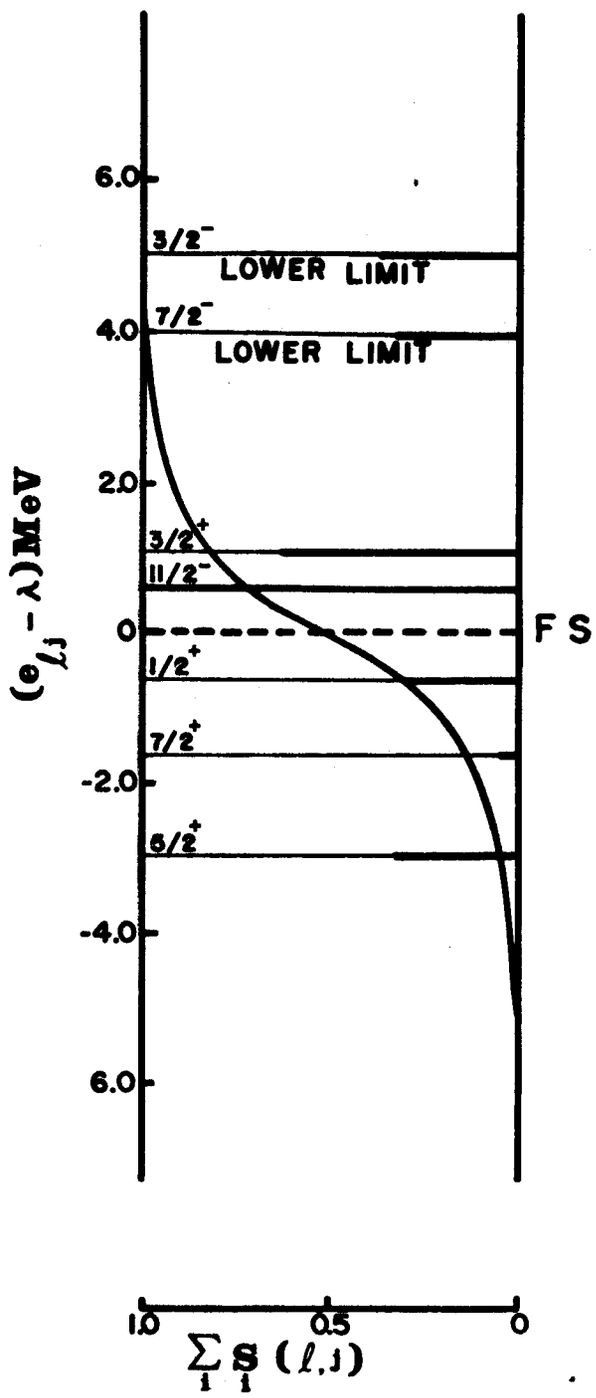
6.0
4.0
2.0
0
-2.0
-4.0
6.0
3/2⁻
LOWER LIMIT
7/2⁻
LOWER LIMIT
3/2⁺
11/2⁻
F S
1/2⁺
7/2⁺
5/2⁺
$(e_{lj} - \lambda)$MeV
1.0
0.5
0
$\sum_i S_i(l,j)$